Shortfin Mako (*Isurus oxyrinchus*)

Supplementary Information for *Isurus oxyrinchus*

Rigby, C.L., Barreto, R., Carlson, J., Fernando, D., Fordham, S., Francis, M.P., Jabado, R.W., Liu, K.M., Marshall, A., Pacoureau, N., Romanov, E., Sherley, R.B. & Winker, H.

To analyse the *Isurus oxyrhincus* population trend data, we used a Bayesian state-space tool for trend analysis of abundance indices for IUCN Red List assessment (Just Another Red List Assessment, JARA), which builds on the Bayesian state-space tool for averaging relative abundance indices by Winker *et al*. (2018).The relative abundance or the population follows an exponential state-space population model of the form: $\mu_{t+1} = \mu_t + r_t$, where μ_t is the logarithm of the expected abundance in year *t,* and r_t is the normally distributed annual rate of change with mean $\bar{r}$, the estimable mean rate of change for a population, and process variance σ^2. We linked the logarithm of the observed relative abundance $I_{t,i}$ for index i (where multiple datasets were available for the same fishery or region) to the expected abundance trend $\log(\hat{I}_t) = \mu_t$ using the observation equation (eqn. 16) from Winker *et al*. (2018). We used a non-informative normal prior for $\bar{r} \sim N(0,1000)$. Priors for the process variance can be either fixed or estimated (see Winker *et al*. 2018 for details). If estimated (default), the priors were $\sigma^2 \sim 1/gamma(0.01,0.01)$, or approximately uniform on the log scale (e.g. Chaloupka and Balazs 2007). Three Monte Carlo Markov chains were run and initiated by assuming a prior distribution on the initial state centred around the first data point in each abundance time series $(y_{t=1})$, $\mu_1 \sim N(\log(y_1),1000)$. The first 20,000 iterations were discarded as burn-in, and of the remaining 200,000 iterations, 100,000 were selected for posterior inference. Thus, posterior distributions were estimated from 300,000 iterations. Analyses were performed using the R Statistical Software v3.5.0 (R Core Team 2018), *via* the interface from R ('r2jags' library v 0.5-7; Su and Yajima 2015) to JAGS ('Just Another Gibbs Sampler' v4.3.0; Plummer 2003). Convergence was diagnosed using Geweke's diagnostic (Geweke 1992) with thresholds of *p* = 0.05, via the 'coda' library (v0.19-1; Plummer *et al.* 2006).

The percentage change *D%* was directly calculated from the posteriors of the estimated population time series $\hat{I}_t$. If the span of $\hat{I}_t$ was longer than 3 x generation length (GL), the percentage change was automatically calculated as the difference between a three-year average around the final observed data point *T*, and a three-year average around the year corresponding to *T*−(3 × GL). The year *T+1* is always projected to obtain a three-year average around *T*. We used a three-year average to reduce the influence of short-term fluctuation (Froese *et al.* 2017). If the span of $\hat{I}$ was shorter than 3 × GL,

JARA projected forward, by passing the number of desired future years without observations to the model, to attain an $\widehat{I_t}$ that spans 3 × GL + 2 years for the calculation of $D\%$. These projections (shown as red dashed lines in the figures below) were based on the posteriors of the estimated decline across all n years in the observed time series: $\bar{r} = \frac{1}{n}\sum_{t=1}^{n} r_t$. The projection gives similar results to extrapolating backwards to attain a 3 x GL period and produces a similar result for the D%.

We analysed the time series for each region where data were available, to produce a) a model fit to the observed data (e.g. Figure 1A), b) an annual rate of change (λ) based on the observed data ($\lambda = \exp(\bar{r})$, expressed as a % in e.g. Figure 1B), c) if needed, projected values for each year necessary to extend the time-series to 3 × GL (e.g. Figure 1C), and d) the posterior distribution for the regional rate of change (%) over 3 × GL (e.g. Figure 1D). Because the posterior distribution comprises an estimated % population change over 3 × GL for each model iteration, these automatically map to the IUCN Red List categories. For example, under criterion A2, an iteration yielding a % population change of +55% would be assigned to the Least Concern category, while iterations giving −82% and −55% would be assigned to Critically Endangered and Endangered, respectively. By assigning the posterior decline from each iteration in this way, it was possible to determine the most likely IUCN Red List category for each region separately (Table 1).

We then assessed the species globally (e.g. Figure 5) by calculating the expected rate of change (%) using the posterior probabilities for each of the regional rates of change weighted by an area-based estimate of the size of each region as a proportion of the species' global distribution. The current distribution map was used to calculate areas (Ebert *et al.* 2013). For any region where the species is known to occur, we sub-sampled (without replacement) from the posterior probability distribution for the regional rate of decline according to the proportion of the total area of a species' distribution that fell within that region. Where a species is known to occur in a region, but no regional trend data were available, we sampled from a uniform distribution, $U(-100,0)$ with the sample size determined by the proportion of the total area of the species' distribution that is contained within those regions.

Table 1. *Isurus oxyrinchus* – Population change (%) and posterior probabilities for changes falling within the IUCN Red List categories Least Concern (LC), Near Threatened (NT), Vulnerable (VU), Endangered (EN), and Critically Endangered (CR); the "likely status" based on criteria A2–4 is assigned based on the category containing the highest posterior probability, with the exception that VU is also selected where LC obtained the highest probability, but it is < 50%. All probabilistic statements are based on the rate of change over three generation lengths (GL) from projections within JARA. The Global change is based on weighting the regional posterior probabilities by the proportional area (PA) weighting (see text for detail).

Region	GL (years)	Data length (years)	PA weighting	Median change	LC	NT	VU	EN	CR	Likely status
Atlantic[1]	25	68	0.29	-60.0	0	0.1	9.9	**90.0**	0	**EN**
N. Pacific[2]	24	42	0.31	-36.5	20.9	15.6	**43.3**	20.3	0	**VU**
S. Pacific[3]	24	19	0.22	+35.2	**69.4**	4.2	9.0	13.4	3.9	**LC**
Indian[4]	24	45	0.18	-47.9	4.5	7.6	**44.3**	43.6	0	**VU**
Global	—	—	—	**-46.6**	22.5	7.2	26.1	**43.3**	0.9	**EN**

Data sources:

1. ICCAT (2017): Figure 2a, BSP2-JAGS biomass, page 23;

2. ISC (2018): Figure ES4, page 12;

3. Francis *et al*. (2014): Figure 25, right panel, page 43;

4. Brunel *et al*. (2018): Figure 6B, page 14

Atlantic: Stock Assessment (1950–2017), north Atlantic, biomass (B/Bmsy).
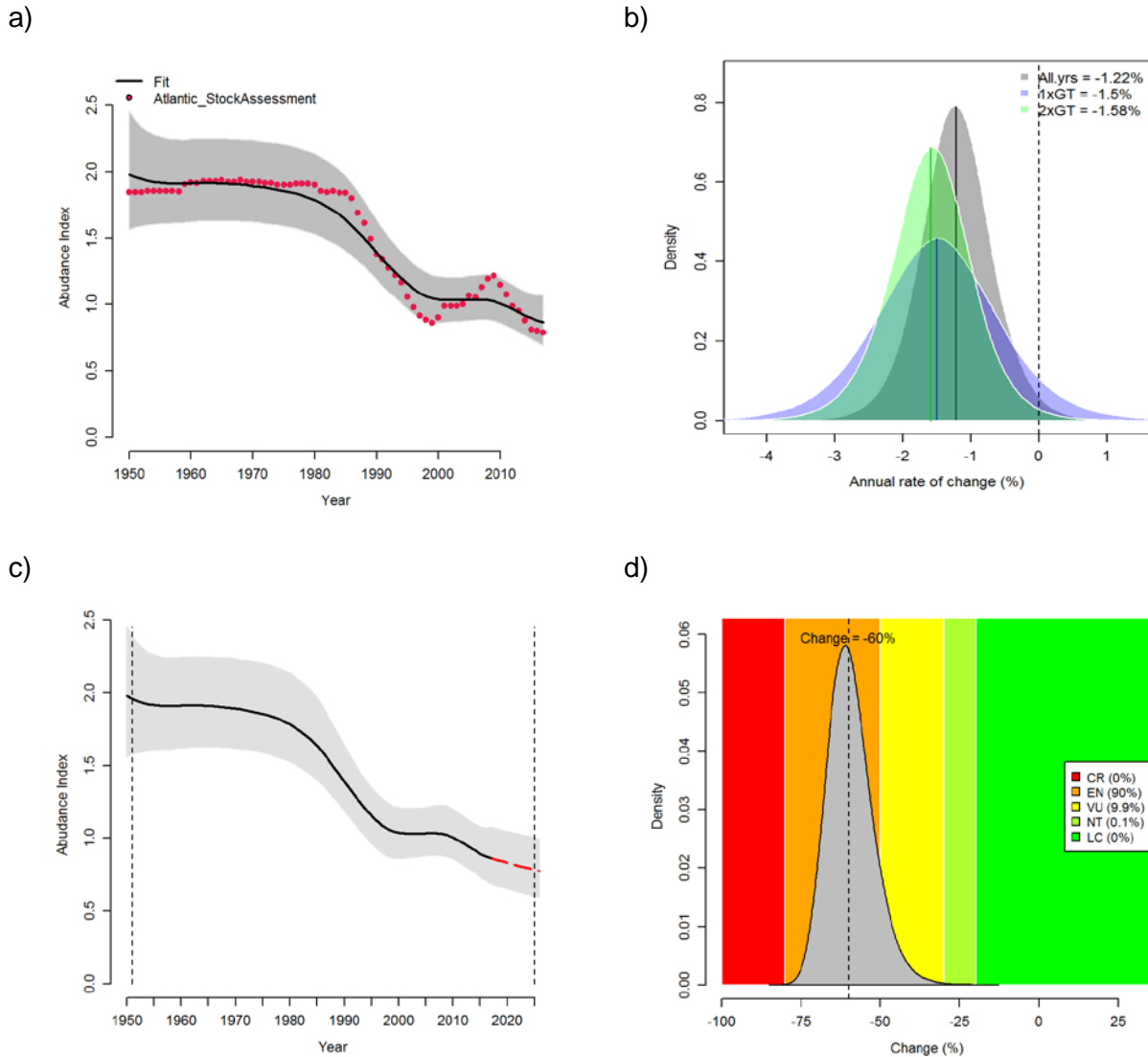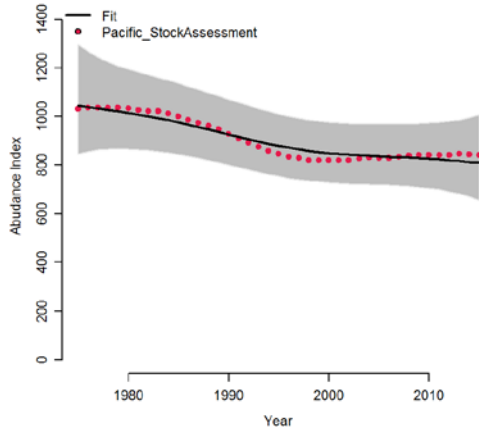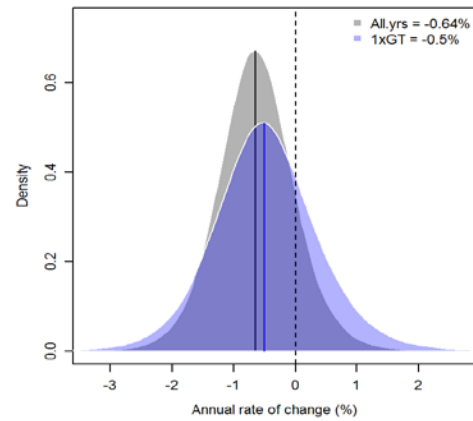
a)

b)

c)

d)

Figure 1. JARA results for *Isurus oxyrinchus* in the Atlantic showing (a) the JARA fit to the observed time-series, (b) the posterior probability for the percentage annual population change calculated from all the observed data (in black), from the last 1 generation length of data (in blue) and from the last 2 generation lengths of data (in green), with the mean (solid lines) shown relative to a stable population (% change = 0, black dashed line), (c) the observed (black line) and predicted (red line) population trajectory over three generations (75 years, dashed grey lines), and (d) the median decline over three generation lengths (dashed line) and corresponding probabilities for rates of population decline falling within the IUCN Red List category.

North Pacific: Stock Assessment (1975–2016), north Pacific, spawning abundance (1000s of sharks-number of mature females).
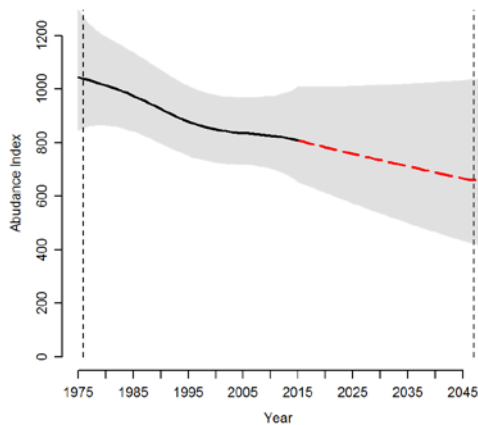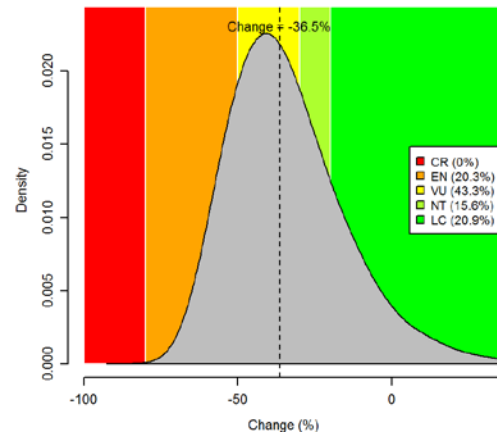
a)

b)

c)

d)

Figure 2. JARA results for *Isurus oxyrinchus* in the North Pacific showing (a) the JARA fit to the observed time-series, (b) the posterior probability for the percentage annual population change calculated from all the observed data (in black) and from the last 1 generation length of data (in blue), with the mean (solid lines) shown relative to a stable population (% change = 0, black dashed line), (c) the observed (black line) and predicted (red line) population trajectory over three generations (72 years, dashed grey lines), and (d) the median decline over three generation lengths (dashed line) and corresponding probabilities for rates of population decline falling within the IUCN Red List category.

South Pacific: CPUE (1995–2013), south Pacific, New Zealand observer based longline (catch per thousand hooks).
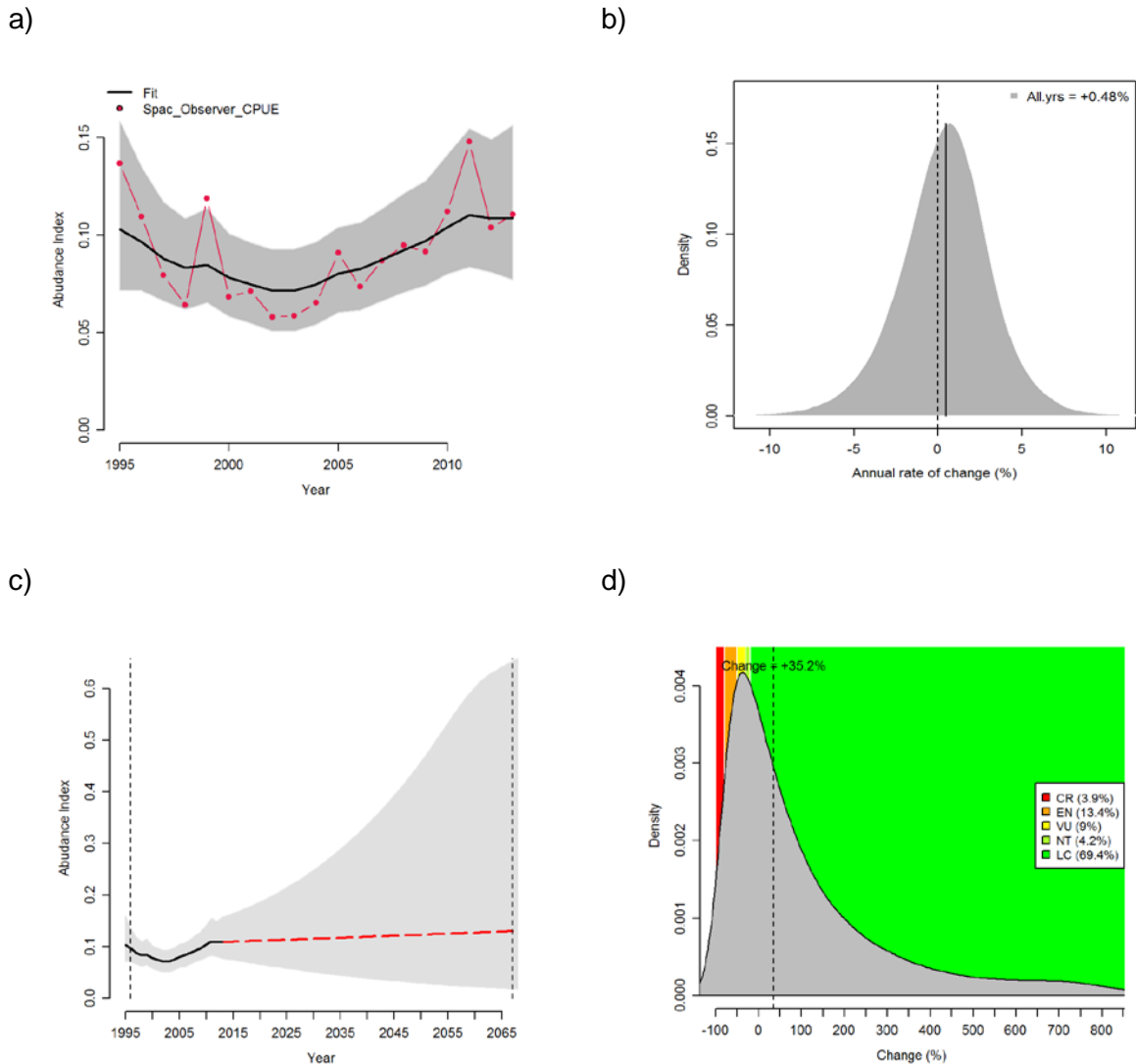
a)

b)

c)

d)

Figure 3. JARA results for *Isurus oxyrinchus* in the south Pacific showing (a) the JARA fit to the observed time-series, (b) the posterior probability for the percentage annual population change calculated from all the observed data (in black), with the mean (solid lines) shown relative to a stable population (% change = 0, black dashed line), (c) the observed (black line) and predicted (red line) population trajectory over three generations (72 years, dashed grey lines), and (d) the median decline over three generation lengths (dashed line) and corresponding probabilities for rates of population decline falling within the IUCN Red List category. In this part of the south Pacific, the level of fishing that was causing a threat is now sustainable, and the Criterion A1 is relevant. However, for a global assessment there is a requirement to apply the criteria consistently at a regional and global level, and at a global level the threats have not ceased, and A2 criteria is appropriate.

Indian: Stock Assessment (1971–2015), IOTC (biomass).
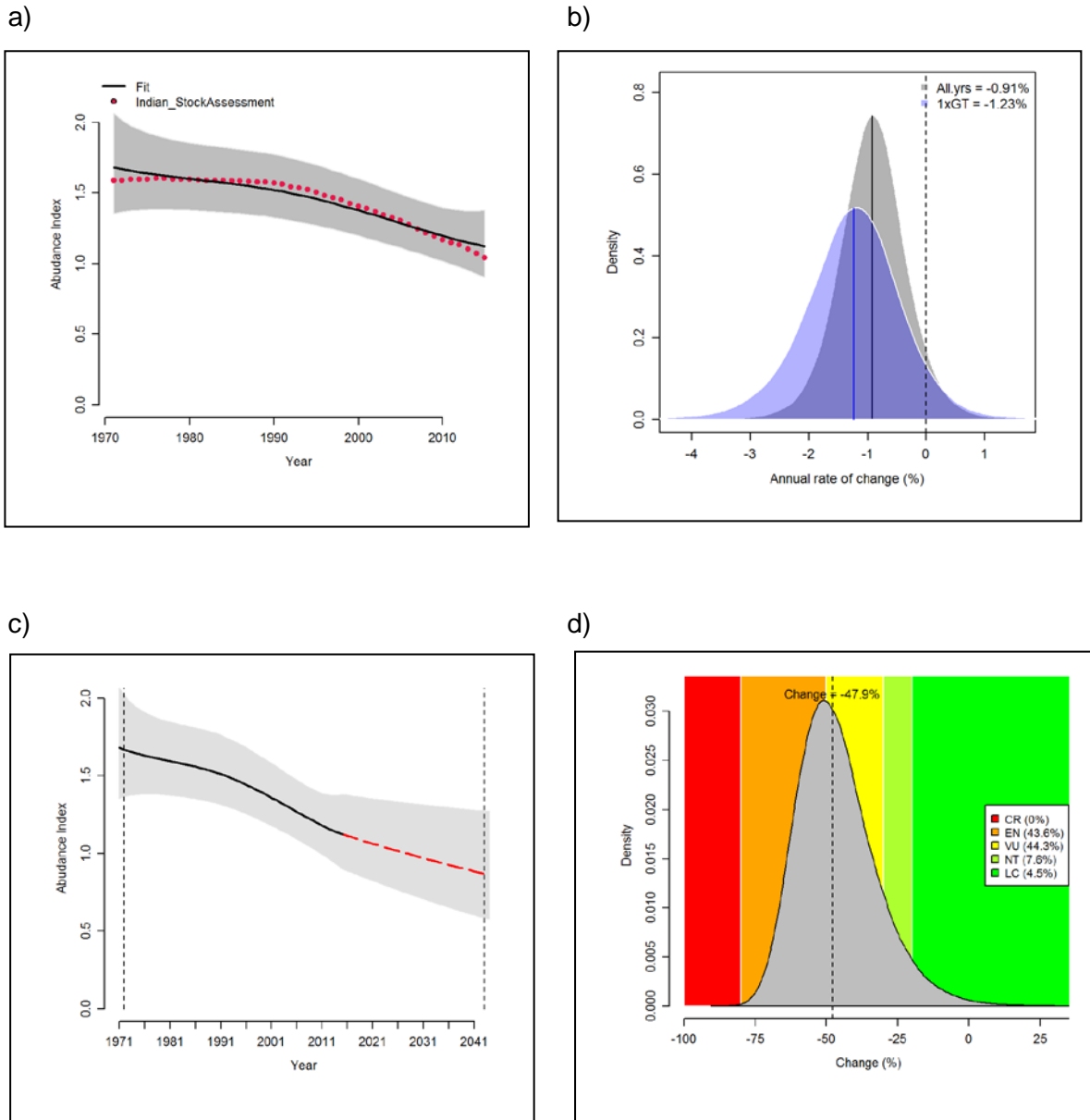
a)

b)

c)

d)

Figure 4. JARA results for *Isurus oxyrinchus* in the Indian Ocean showing (a) the JARA fit to the observed time-series, (b) the posterior probability for the percentage annual population change calculated from all the observed data (in black) and from the last 1 generation length only (in blue), with the mean (solid lines) shown relative to a stable population (% change = 0, black dashed line), (c) the observed (black line) and predicted (red line) population trajectory over three generations (72 years, dashed grey lines), and (d) the median decline over three generation lengths (dashed line) and corresponding probabilities for rates of population decline falling within the IUCN Red List category.

Global weighted trend:

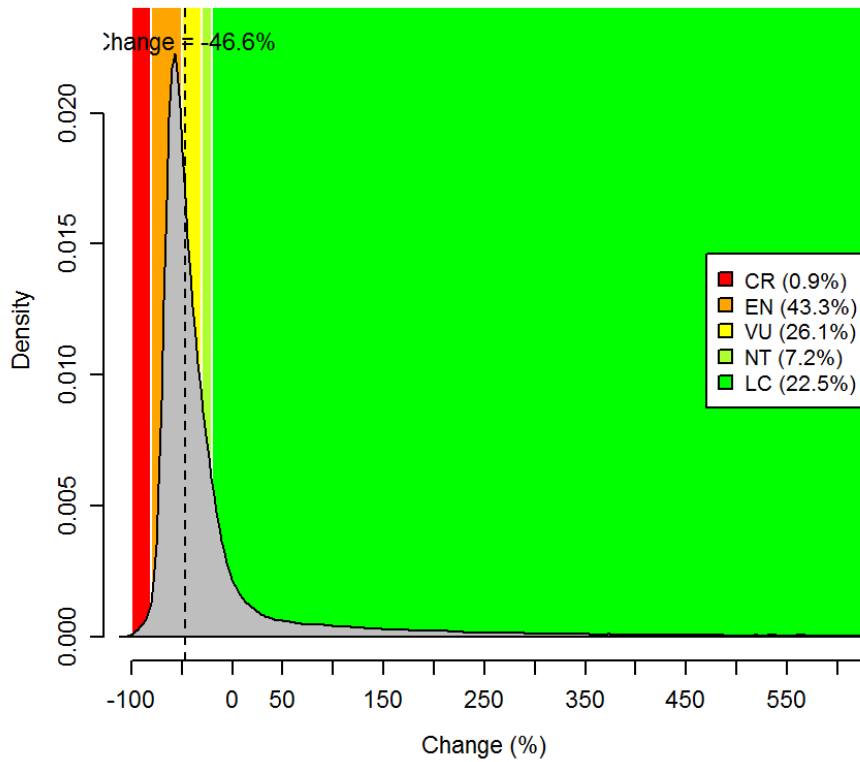Median (95% CI) change = −46.6% (−71.7–357.1%).

Figure 5. Global weighted trend for *Isurus oxyrinchus* based on weighting the regional posterior probabilities for the rates of population decline over three generations by the relative area of each region as a proportion of the species' global distribution.

References

Brunel, T., Coelho, R., Merino, G., Ortiz de Urbina, J., Rosa, D., Santos, C., Murua, H., Bach, P., Saber, S. and Macias, D. (2018) A preliminary stock assessment for the shortfin mako shark in the Indian Ocean using data-limited approaches. IOTC-WPEB14-2018-037.

Chaloupka, M. and Balazs, G. (2007) Using Bayesian state-space modelling to assess the recovery and harvest potential of the Hawaiian green sea turtle stock. *Ecological Modelling* 205: 93–109.

Ebert, D.A., Fowler, S., Compagno, L. and Dando, M. (2013). *Sharks of the World: A fully Illustated Guide*. Wild Nature Press, Plymouth.

Francis, M.P., Clarke, S.C., Griggs, L.H and Hoyle, S.D. 2014. Indicator based analyses of the status of New Zealand blue, mako and porbeagle sharks. New Zealand Fisheries Assessment Report 2014/69. Ministry for Primary Industries.

Froese, R., Demirel, N., Coro, G., Kleisner, K.M. and Winker, H. (2017) Estimating fisheries reference points from catch and resilience. *Fish and Fisheries* 18: 506–526.

Geweke, J. (1992) Evaluating the accuracy of sampling-based approaches to the calculation of posterior moments. In: *Bayesian Statistics 4: Proceedings of the Fourth Valencia International Meeting.* (eds J.O. Berger, J.M. Bernardo, A.P. Dawid and A.F.M. Smith). Clarendon Press, Oxford, pp 169–193.

ICCAT (2017) Report of the 2017 ICCAT Shortfin Mako Assessment Meeting. Madrid, Spain 12-16 June 2017.

ISC (2018) Stock Assessment of Shortfin Mako Shark (*Isurus oxyrinchus)* in the Pacific Ocean Through 2016. WCPFC Northern Committee 14th Regular Session. WCPFC-NC14-2018/IP-06, Fukuoka, Japan, 118 pp.

Lawson, J.M., Fordham, S.V., O'Malley, M.P., Davidson, L.N.K., Walls, R.H.L., Heupel, M.R., Stevens, G., Fernando, D., Budziak, A., Simpfendorfer, C.A., Ender, I., Francis, M.P., Notarbartolo di Sciara, G., and Dulvy, N.K. (2017) Sympathy for the devil: a conservation strategy for devil and manta rays. *PeerJ* 5: e3027.

Plummer M. 2003. JAGS: A program for analysis of Bayesian graphical models using Gibbs sampling. Proceedings of the 3rd International Workshop on Distributed Statistical Computing. https://www.r-project.org/conferences/DSC-2003/Proceedings/Plummer.pdf

Plummer, M., Nicky Best, Cowles, K. and Vines, K. (2006) CODA: Convergence Diagnosis and Output Analysis for MCMC. *R News* 6: 7–11.

Su, Y.-S. and Yajima, M. (2015) R2jags: Using R to Run 'JAGS'. R package version 0.5-7. https://CRAN.R-project.org/package=R2jags.

Winker, H., Carvalho, F. and Kapur, M. (2018) JABBA: Just Another Bayesian Biomass Assessment. *Fisheries Research* 204: 275–288.

Winker H., Carvalho, F., Sharma, R., Parker, D. and Kerwath, S. (2017). Initial results for North and South Atlantic Shortfin Mako (*Isurus oxyrinchus)* stock assessment using the Bayesian surplus production model *JABBA* and the Catch-Resilience Method *CMSY*. *International Commission for the Conservation of Atlantic Tunas Collective Volume of Scientific Papers* 74: 18361–866.